



Adsorption and photocatalysed destruction of cationic and anionic dyes on mesoporous titania films: Reactions at the air–solid interface

Andrew Mills ^{*}, Mubeen Sheik, Christopher O'Rourke, Michael McFarlane

Department of Pure & Applied Chemistry, University of Strathclyde, 295 Cathedral Street, Glasgow, G1 1XL, United Kingdom

ARTICLE INFO

Article history:

Received 15 November 2008

Accepted 22 November 2008

Available online 30 November 2008

Keywords:

Photocatalysis

Dye

Methylene blue

Acid orange 7

Adsorption

Air–solid

ABSTRACT

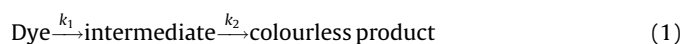
Cationic dyes, such as methylene blue (MB), Thionine (TH) and Basic Fuschin (BF), but not anionic dyes, such as Acid Orange 7 (AO7), Acid Blue 9 (AB9) and Acid Fuschin (AF), are readily adsorbed onto mesoporous titania films at high pH (pH 11), i.e. well above the pzc of titania (pH 6.5), due to electrostatic forces of attraction and repulsion, respectively. The same anionic dyes, but not the cationic dyes, are readily adsorbed on the same titania films at low pH (pH 3), i.e. well below titania's pzc. MB appears to adsorb on mesoporous titania films at pH 11 as the trimer ($\lambda_{\text{max}} = 570 \text{ nm}$) but, upon drying, although the trimer still dominates, there is an absorption peak at 665 nm, especially notable at low [MB], which may be due to the monomer, but more likely MB J-aggregates. In contrast, the absorption spectrum of AO7 adsorbed onto the mesoporous titania film at low pH is very similar to the dye monomer. For both MB and AO7 the kinetics of adsorption are first order and yield high rate constants (3.71 and $1.48 \text{ l g}^{-1} \text{ min}^{-1}$), indicative of a strong adsorption process. Indeed, both MB and AO7 stained films retained much of their colour when left overnight in dye-free pH 11 and 3 solutions, respectively, indicating the strong nature of the adsorption. The kinetics of the photocatalytic bleaching of the MB–titania films at high pH are complex and not well-described by the Julson–Ollis kinetic model [A.J. Julson, D.F. Ollis, *Appl. Catal. B.* 65 (2006) 315]. Instead, there appears to be an initial fast but not simple demethylation step, followed by a zero-order bleaching and further demethylation steps. In contrast, the kinetics of photocatalytic bleaching of the AO7–titania film give a good fit to the Julson–Ollis kinetic model, yielding values for the various fitting parameters not too dissimilar to those reported for AO7 adsorbed on P25 titania powder.

© 2008 Elsevier B.V. All rights reserved.

1. Introduction

Semiconductor photocatalysis, SPC, is an established, significant and still-expanding area of research which has led to numerous commercial products, such as self-cleaning glass, tiles and paint [2]. The current commercial manifestations of SPC usually utilise a layer of the semiconductor photocatalyst, invariably anatase titania. Methods for assessing and characterising the activities of such films are numerous and varied and include: (i) the photobleaching of a dyestuff, such as methylene blue (MB), or acid orange 7 (AO7), dissolved in aqueous solution [3,4], (ii) the photomineralisation of a thin solid film of a wax-like substance, such as stearic or palmitic acid [5,6] and, (iii) the photo-oxidation of a gas phase pollutant, such as nitric oxide or acetaldehyde [7,8]. Neither of these tests are particularly fast or inexpensive to run; nor are they conducive to ready demonstration.

One route towards demonstrating the photocatalytic action of films is to deposit the dye directly onto the surface and monitor the photobleaching process at the air–solid interface. Recently, Julson and Ollis have shown that sufficient dye (such as acid blue 9 (AB9), AO7, reactive black and reactive blue can be adsorbed onto a P25 titania photocatalyst powder by just stirring the two together overnight [1]. The filtered, dried, dye-stained powder can then be used to study dye decolourisation kinetics at the air–solid interface. This work was later extended by the same group to include Pilkington ActivTM, a commercial self-cleaning glass which uses a 15 nm thick film of titania photocatalyst film as its active layer [9]. For both systems the kinetics of dye photobleaching are well described by two first-order reactions coupled in series, with the first the conversion of the dye to a less-coloured intermediate and the second the subsequent conversion of the intermediate to a colourless product [1,9], i.e.



where k_1 and k_2 are the first order rate constants.

^{*} Corresponding author.

E-mail address: a.mills@strath.ac.uk (A. Mills).

The most obvious route to depositing dyes on titania *films* is dip-coating [9], although this tends to produce multilayered (>40 layers) films of the dye [9]. An alternative, possibly less crude, method of depositing monolayer films of dyes on the surface of titania is suggested by the work of Herrmann and co-workers in their study of the photodegradation of dyes, such as Alizarin S, Crocein Orange G (OG), Methyl Red, Congo Red and MB, by P25 titania *powder* dispersed in solution [10], and involves dye adsorption due to electrostatic attraction. This work reveals that the amount of dye adsorbed depends upon the relative signs and magnitudes of the charges on the dye and the titania particles, with, understandably, most dye being adsorbed when the two are large and of opposite sign. As with all metal oxides the sign and magnitude of the charge on titania is pH dependent. This will also be the case for most dyes under test, given that most will exist in one or more protonated and deprotonated forms at different pHs. Thus, as Herrmann and his colleagues noted [10], most of the anionic dye, OG, is adsorbed onto P25 TiO₂ under acidic conditions (pH 3), when the surface of the titania is positively charged, and most of the cationic dye, MB, is adsorbed under alkaline conditions (pH 9), when the surface of the titania is negatively charged; the pzc of titania being pH 6.5 [11].

It follows from this excellent work on titania *powders*, that *films* of titania, especially macro and mesoporous films, should be readily and visibly stained by such cationic dyes, under alkaline conditions, and by anionic dyes, under acidic conditions. This paper reports the results of an investigation into this route to dye deposition using thick, mesoporous titania films, and a subsequent study of the kinetics of photocatalytic destruction of two such, dried, stained films. This work is novel, not least because the literature on the photocatalytic destruction of adsorbed dyes in air–solid systems is ‘modest’ [1], and there are few reports on dry, dye-photocatalyst *films*, despite their importance not only as an easily monitored test system, but also as a possible demonstrator of photocatalytic activity.

2. Experimental

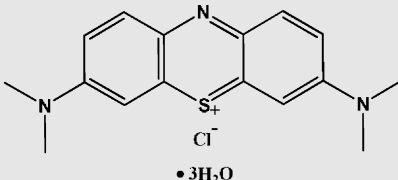
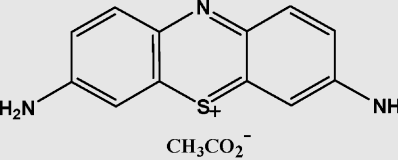
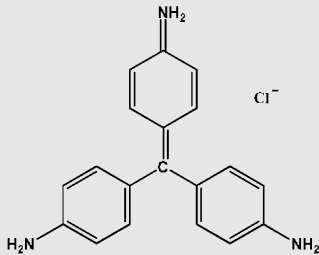
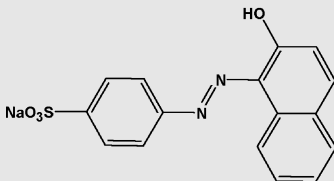
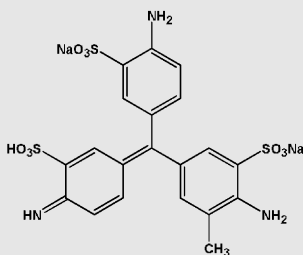
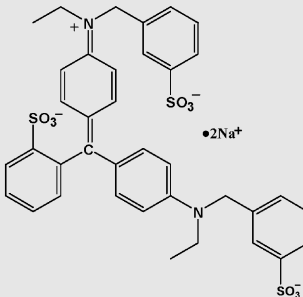
All chemicals were purchased from Aldrich Chemicals and used as received, unless stated otherwise. The thick (1.8 μm) mesoporous (overall porosity ca. 55%; specific surface area ca. 64 $\text{m}^2 \text{g}^{-1}$) anatase titania films used throughout this work were prepared via a sol gel, hydrothermal process, as described in detail elsewhere [12]. Briefly 4.65 g of acetic acid were added to 20 ml of titanium isopropoxide under an inert nitrogen atmosphere. To this were added 120 ml of 0.1 mol dm^{-3} nitric acid and, after mixing the reaction solution, was heated rapidly to 80 °C whereupon it turned milky white and opaque. Within a few minutes at this temperature the reaction solution gelled but became fluid again within 1–2 h. The reaction solution was maintained at 80 °C for 8 h whereupon it was allowed to cool to room temperature and any remaining aggregate particles were removed using a 0.45 m syringe filter. 80 ml of the colloidal solution were then placed in a Teflon pot with lid in an autoclave (Parr Instruments, UK) and heated and maintained at 220 °C for 12 h. Upon removal of the solution from the autoclave the separated out colloidal particles were redispersed using ultrasound. The reaction solution was then concentrated to about 12 wt.% using a rotary evaporator, followed by the addition of 50 wt.% Carbowax 20 M to help prevent the formation of small surface cracks when the paste is cast and allowed to dry. The final form of the titanium dioxide paste is a white, mayonnaise-like, substance which is stable for many months when kept in the fridge. The films were coated on 25 mm^2 borosilicate microscope glass substrates, by placing a few drops of the titania paste onto the substrate, held down by two Sellotape™ tracks, ca. 2 cm apart and drawing it down using a doctor blade

technique. The film was then annealed at 450 °C for 30 min and then cooled down in air.

Dye adsorption was carried out by placing the films in a stirred aqueous solution, at either low pH (pH 3; 10^{-3} M HCl) or high pH (pH 11; 10^{-3} M NaOH), containing the dye of interest at a known concentration, for 10 min, followed by rapid removal and drying flat using an air stream of 60 l min^{-1} . UV/visible absorption spectra and all absorbance vs time experiments were recorded using a

Table 1

Dye names, abbreviations, structures and pK_a 's.

Dye (abbreviation)	Structure	pK_a
Methylene Blue (MB)		0
Thionin (TH)		11
Basic Fuchsin (BF)		2.9
Acid Orange 7 (AO7)		8.3, 11.4
Acid Fuchsin (AF)		13
Acid Blue 9 (AB9)		–

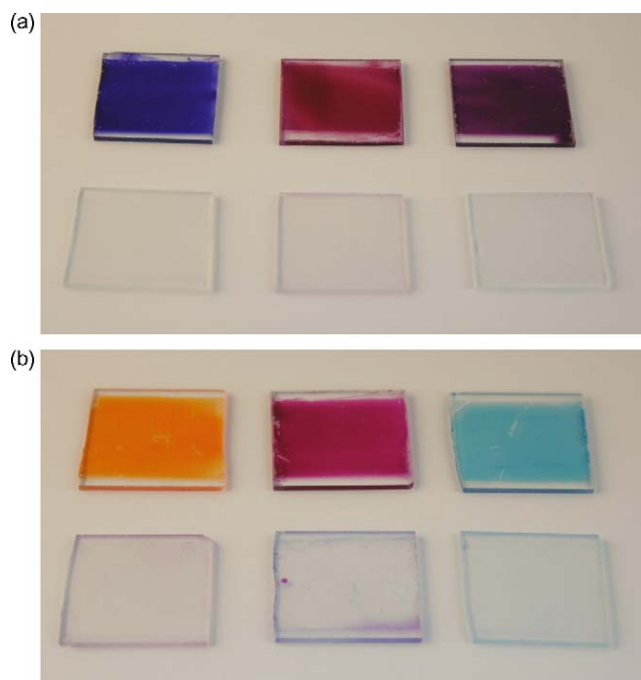


Fig. 1. Two photographs of thick, mesoporous films of titania stained with (top three left to right): MB, TH and BF, and (bottom three left to right): AO7, AF and AB9, respectively, at (a) pH 11 and (b) pH 3. To create the stained films the titania films were soaked in the dye solution under test (0.6 g l^{-1}) for 10 min and then air-dried rapidly.

Shimadzu UV-1800 UV/vis spectrophotometer. All irradiations were carried out using two 8 W UVA (black–light blue) lamps, with each sample placed square on, 2 cm from the light source, and so exposed to an incident light irradiance of ca. 5 mW cm^{-2} , as measured using a UVX radiometer power meter with UVA (UVX-36; UVP) sensor. All photographs were taken with a Canon EOS 350D digital camera.

3. Results and discussion

3.1. Dye adsorption

The dyes used to stain the thick, porous titania films were: MB, thionine (TH), Basic Fuschin (BF), AO7, Acid Fuschin (AF) and AB9; the structures and relevant pK_a 's for these dyes are given in Table 1 [13,14]. At the high and low pH's used in the deposition process in this work the first three of these dyes can be considered as cationic and the last three anionic. In a simple set of experiments, a fresh titania film was placed in a stirred solution, at either pH 3 or 11, containing the dye under test (0.6 g l^{-1}) and, after 10 min soaking, rapidly removed and dried. Photographs of the final dried films are illustrated in Fig. 1(a) and show that at high pH, the cationic dyes: MB, TH and BF are adsorbed to a significant extent onto the titania, whereas the anionic dyes, AO7, AF and AB9 are not and that these roles are reversed at low pH, see Fig. 1(b).

These results indicate that adsorption of the selected dyes on the titania films at these extremes in pH is dominated by electrostatic effects, as found by Herrmann and his co-workers when using P25 powder [10]. For example, at the high pH, the titania film will be negatively charged due to deprotonation of the surface hydroxyl groups, i.e.



And it follows that at this pH, on electrostatic grounds at least, the cationic dyes: MB, TH and BF will be strongly adsorbed onto the

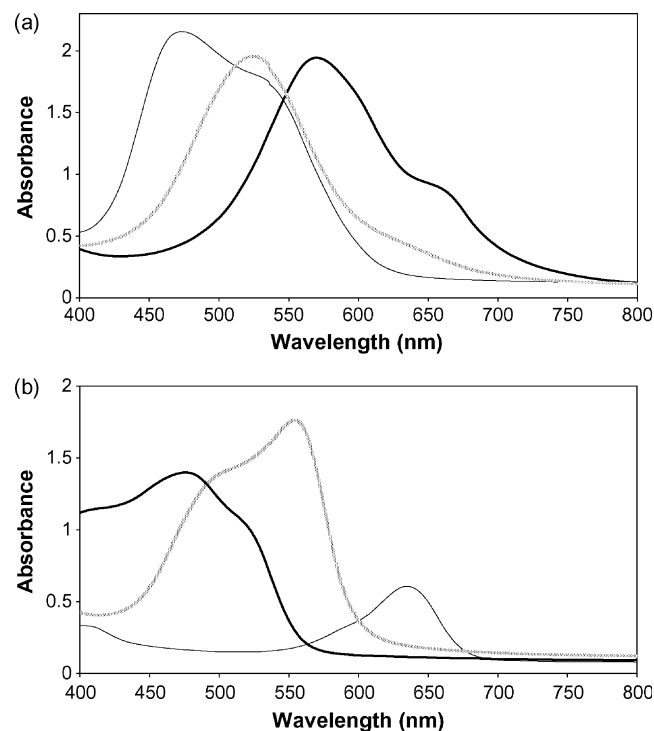


Fig. 2. Visible absorption spectra of the coloured films photographed in Fig. 1. (a) At pH 11, the spectra correspond to coloured films stained with (from left to right): BF, TH and MB, whereas, (b) at pH 3 they correspond to (from left to right) AO7, AF and AB9 stained films.

negatively charged surface of titania, whereas the anionic ones, AO7, AF and AB9, will not, which is as observed, see Fig. 1(a). The dye adsorption results observed at low pH, see Fig. 1(b), can be similarly justified, since at this pH the titania film will be positively charged due to protonation of the surface hydroxyl groups, i.e.



And at this pH, the sulfonic acid groups present in AO7, AF and AB9 will still be deprotonated, making the dyes negatively charged and attracted to the positive surface of the titania film. In contrast, MB, TH and BF will be positively charged and repulsed from the titania surface and so only weakly, if at all, adsorbed. These results on nanocrystalline titania films also appear consistent with those of Herrmann and co-workers working with MB and P25 titania powder [15], although they found MB still to be adsorbed significantly on P25 at pH 3 ($0.75 \text{ mg MB/g TiO}_2$), and that this value only increased 2.1 times upon changing to pH 9. In striking contrast, as indicated by the results in Fig. 1, when using thick, mesoporous titania films, instead of powders, there is little evidence of adsorption of MB, TH and BF at pH 3 or AO7, AF and AB9 at pH 11, i.e. electrostatic effects on dye adsorption appear more significant with these mesoporous films.

The UV/visible absorption spectra of the dye-stained, dry titania films are illustrated in Fig. 2 and reveal that MB adsorbs mainly as the trimer, given $\lambda_{\text{max}} = 570\text{--}575 \text{ nm}$ for the dried film and λ_{max} for the trimer, dimer and monomer of MB are $= 578, 606$ and 665 nm respectively [16]. This observation is not too surprising given the high dye concentration ($0.6 \text{ g l}^{-1} \equiv 1.6 \text{ mM MB}$) and significant dimerisation and trimerisation constants for MB in water ($2 \times 10^3 \text{ M}^{-1}$ and $6 \times 10^6 \text{ M}^{-2}$ at 30°C respectively) [18]. Indeed, based on these constants, the calculated fractional levels of monomer, dimer and trimer of MB at 1.6 mM will be: 0.22, 0.3 and 0.48, respectively. Not surprisingly, given its structural similarity, TH behaves in a similar fashion to MB, thus λ_{max} ($=525 \text{ nm}$) of its

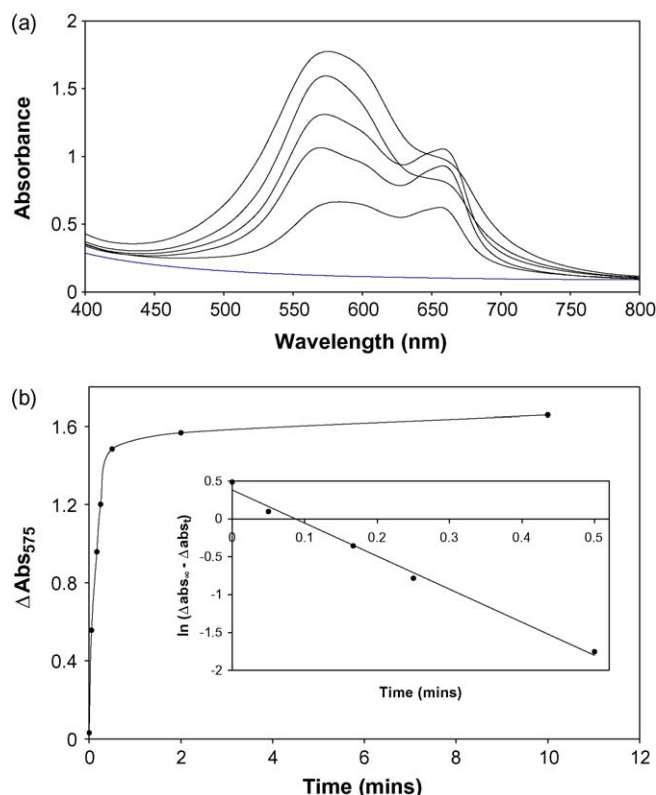


Fig. 3. (a) Variation in the visible absorption spectrum of a titania film stained with MB (0.6 g l^{-1}) for (from bottom to top): 0, 3, 10, 15, 30 and 600 s, respectively. (b) Variation of ΔAbs_{575} as a function of soaking time generated using the data in Fig. 3(a) as well as that from additional experiments. The insert diagram is a first order plot of the data in the main diagram with a line of best fit of gradient = -4.4 min^{-1} .

adsorbed form is, like MB, significantly blue-shifted compared to that of its monomer in aqueous solution ($\lambda_{\text{max}} = 599 \text{ nm}$), and is probably also mostly present as its trimer. Interestingly, BF also forms such H-aggregates on the surface of titania (with $\lambda_{\text{max}} = 474 \text{ nm}$) and yet the concentrated staining solution ($0.6 \text{ g l}^{-1} \equiv 1.9 \text{ mM}$ BF) has the same spectral profile as the monomer ($\lambda_{\text{max}} = 546 \text{ nm}$). The latter feature is found for the remaining dyes (AO7, AF and AB9) and when adsorbed onto titania under acidic conditions their spectral profiles are much like their monomeric forms with $\lambda_{\text{max}} = 486, 540$ and 629 nm , respectively.

The kinetics of the electrostatic-driven adsorption process were studied in more detail for two of the dyes used above, namely MB (at high pH) and AO7 (at low pH) and the results of this work are reported below.

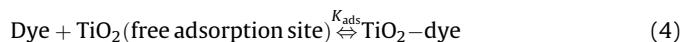
3.2. Kinetics of MB and AO7 adsorption

As we have seen, at high pH MB adsorbs readily onto TiO_2 to form highly coloured films, thus, the kinetics of this process can be assessed by monitoring the change in the absorbance spectrum of the dried titania film as a function of soaking time (0.6 g l^{-1} MB solution at pH 11) and the results of this work are illustrated in Fig. 3(a). Comparison of these spectra with those reported for the monomer, dimer and trimer forms of MB [16] suggests that in the first 15 s, the dye dries onto the film as a mixture of monomer (ca. 14%) and trimer (ca. 86%) species, with very little dimer present—which seems unlikely. Much longer adsorption time appears to lead to an increased level of trimer (ca. 91% after 10 min) at the apparent expense of the monomer (ca. 8%). Although it is possible that the monomer form of MB exists on the dried film, presumably

due to adsorption at sterically hindered sites that are only able to accommodate such a species, an alternative, more plausible explanation for the significant absorbance at 665 nm is that the MB dimers in solution adsorb on the surface of the titania primarily as J-aggregates, i.e. end-to-end type, rather than as the usual sandwich type, H-aggregates found in aqueous solution. J-aggregates of MB have been reported previously by others, using aqueous solutions of urea, and exhibit a spectral profile and λ_{max} very similar to that of the monomer [17].

For most dried MB films the predominant species is the trimer with its peak at λ_{max} at 575 nm and this dominant peak provides a handle with which to assess the kinetics of adsorption of MB by studying the variation in the change in absorbance at 575 nm of the dried, stained titania film, i.e. ΔAbs_{575} , as a function of soaking time, using a 0.6 g l^{-1} MB staining solution; the results of this work are illustrated in Fig. 3(b). The adsorption process fits good first order kinetics, as illustrated by the straight line plot of the data in the insert diagram in Fig. 3(b) which yields a gradient, k_{dep} , of 4.4 min^{-1} .

In order to understand better the relevance of the value of k_{dep} , the adsorption process needs to be described in a little more detail. Thus, it is well established that the Langmuir adsorption constant, K_{ads} , for the adsorption process:



has a large value ($6.65 \times 10^3 \text{ M}^{-1}$ at natural pH, i.e. pH 5) when the dye is MB [15], and this value is likely to be even greater when a higher pH, such as in this work, is used. In addition, since

$$K_{\text{ads}} = \frac{k_{\text{ads}}}{k_{\text{des}}} \quad (5)$$

where k_{ads} and k_{des} are the bimolecular and first order rate constants for dye adsorption and desorption, respectively, onto titania, it follows from Eq. (5) that $k_{\text{ads}} \gg k_{\text{des}}$ for the adsorption of MB onto titania. Using this model, the kinetics of adsorption as a function of soaking time, t , are then described by the following expression:

$$[\text{TiO}_2\text{--dye}]_{\infty} - [\text{TiO}_2\text{--dye}]_t = [\text{TiO}_2\text{--dye}]_{\infty} \exp(-k_{\text{ads}}[\text{dye}] + k_{\text{des}}t) \quad (6)$$

where $[\text{TiO}_2\text{--dye}]_{\infty}$ and $[\text{TiO}_2\text{--dye}]_t$ are the concentrations of the dye-occupied adsorption sites at equilibrium and time, t ,

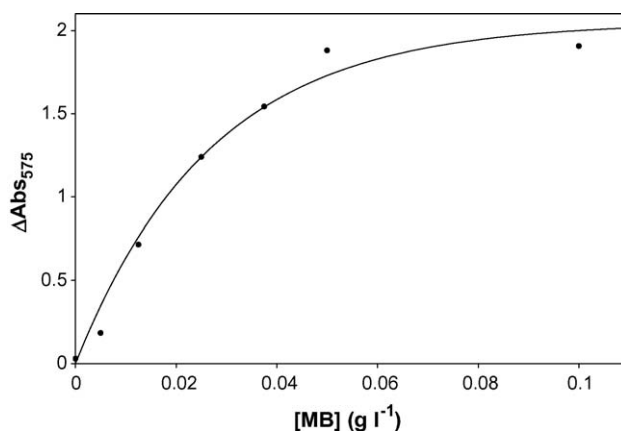


Fig. 4. Plot of ΔAbs_{575} as a function of $[\text{MB}]$, recorded after 10 min soaking in the MB solutions at pH 11 and then rapid drying. The solid line is the line of best fit calculated using Eq. (6), assuming $k_{\text{ads}}[\text{dye}] \approx (k_{\text{ads}}[\text{dye}] + k_{\text{des}})$, and the following optimised values for $\Delta\text{Abs}_{575}(\infty) (\propto [\text{TiO}_2\text{--dye}]_{\infty})$ and k_{ads} of 2.05 and $3.71 \text{ g}^{-1} \text{ min}^{-1}$, respectively.

respectively, and $[\text{dye}]$ is the initial concentration of dye, assuming that the total number of dye-adsorption sites is significantly less than that of dye molecules in the staining solution.

In our work, the experimentally measurable parameters: ΔAbs_{575} , at time t and at equilibrium, $\Delta\text{Abs}_{575}(\infty)$, provide measures of $[\text{TiO}_2\text{-dye}]_t$ and $[\text{TiO}_2\text{-dye}]_\infty$, respectively. It follows that the value of k_{dep} derived from the first-order plot of the data illustrated in Fig. 3(b), i.e. 4.4 min^{-1} , is actually a measure of $(k_{\text{ads}}[\text{dye}] + k_{\text{des}})$. In our system the value of $[\text{dye}]$ is large (0.6 g l^{-1}) and so k_{dep} will be large. In contrast, in the work of Herrmann and co-workers [18], $[\text{dye}]$ is small (0.031 g l^{-1}) and so k_{dep} is much smaller (reported as 0.082 min^{-1}). From the latter results, assuming $K_{\text{ads}} = 6.65 \times 10^3 \text{ M}^{-1}$ [15], it is possible to estimate values for k_{ads} and k_{des} of: $0.94 \text{ l g}^{-1} \text{ min}^{-1}$ and 0.053 min^{-1} at pH 5. In the work reported here, the high $[\text{dye}]$, 0.6 g l^{-1} , makes it likely that $k_{\text{ads}}[\text{dye}] \gg k_{\text{des}}$ and so $k_{\text{dep}} \approx k_{\text{ads}}[\text{dye}]$, from which a value of $k_{\text{ads}} \approx 7.3 \text{ l g}^{-1} \text{ min}^{-1}$ for MB adsorption on titania films at pH 11 can be estimated, i.e. ca. 8 times greater than that estimated using the data of Herrmann and co-workers at pH 5 for MB on P25 TiO_2 powder [18]. This striking difference arises from the much increased coulombic forces of attraction in effect at the higher pH, a good illustration of which is the observation that a freshly stained MB–titania film loses little of its colour ($2.2\% \text{ h}^{-1}$) when placed in a MB-free pH 11 aqueous solution directly after its creation, i.e. the value of K_{ads} is so large at this pH that $k_{\text{ads}}[\text{dye}] \gg k_{\text{des}}$ and the adsorption process appears, initially at least, irreversible.

A better estimate of the value for k_{ads} can be gleaned from a study of the variation in the value of ΔAbs_{575} , after a fixed (10 min in this case) soaking time in MB solutions of different concentrations at pH 11. The measured variation in ΔAbs_{575} as a function of $[\text{MB}]$ is illustrated in Fig. 4, with a solid line of best fit calculated using Eq. (6), assuming $k_{\text{ads}}[\text{dye}] \approx (k_{\text{ads}}[\text{dye}] + k_{\text{des}})$, and the optimised values for $\Delta\text{Abs}_{575}(\infty) (\propto [\text{TiO}_2\text{-dye}]_\infty)$ and k_{ads} of 2.05 and $3.7 \text{ l g}^{-1} \text{ min}^{-1}$, respectively.

A similar set of experiments to those reported above for MB were carried out using AO7 at low pH and like MB, a 0.6 g l^{-1} ($\approx 1.7 \text{ mM}$) staining solution of AO7 appeared to deposit quickly onto a titania film and, as noted earlier, unlike MB, the deposited dried film of AO7 exhibited a spectral profile and λ_{max} ($=477 \text{ nm}$) very similar to that of AO7 in dilute (10^{-5} M , $\lambda_{\text{max}} = 483 \text{ nm}$) solution, i.e. the AO7 appeared to be adsorbed as the monomer.

The adsorption kinetics for AO7 on the titania were probed by studying the variation in the value of ΔAbs_{477} , after a fixed (10 min in this case) soaking time in AO7 solutions of different concentrations at low pH. This work generated the variation in the absorption spectra of the dried, AO7 adsorbed on titania film as a function of the concentration of the AO7 staining solution illustrated in Fig. 5. The measured variation in ΔAbs_{575} as a function of $[\text{AO7}]$, illustrated in the insert diagram in Fig. 5, gave a good fit to Eq. (6), using optimised values for $\Delta\text{Abs}_{477}(\infty) (\propto [\text{TiO}_2\text{-dye}]_\infty)$ and k_{ads} of 1.41 and $1.48 \text{ l g}^{-1} \text{ min}^{-1}$, respectively. The latter value of k_{ads} is ca. 2.5 times less than that for MB, possibly because the coulombic forces of attraction are less for the AO7–titania system since the deviation from titania's pzc (at 6.5) is smaller (3.5 pH units) compared to that for the MB–titania system (4.5 pH units). Using Crocein Orange G, a dye that is very similar in structure to AO7, Herrmann and his co-workers report a value for K_{ads} ($5.64 \times 10^3 \text{ M}^{-1}$) at natural pH on P25 that is 16% lower than that the value they reported for MB [15]. Thus, like OG, it is probable that AO7 is strongly adsorbed on titania and will be more so at pH 3 due to significant coulombic forces of attraction. Like MB at high pH, AO7 at low pH when adsorbed on titania does not lose all its colour over overnight when placed in a AO7-free pH 3 aqueous solution, although it does lose some (5% per h), indicating that the values for K_{ads} and k_{ads} for AO7 at pH 3 are less than those

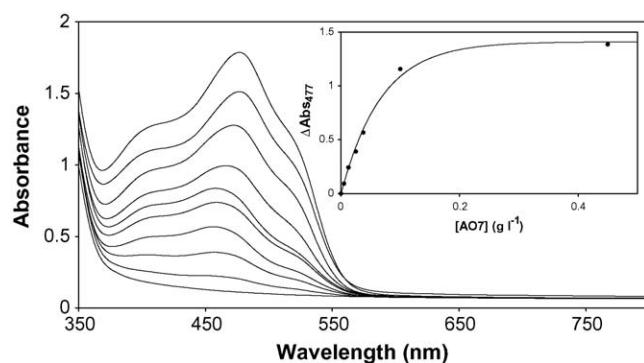


Fig. 5. UV/Vis absorption spectra of the titania films soaked for 10 min in AO7 solutions (pH 3) with the following different concentrations (from bottom to top): 0, 0.005, 0.0125, 0.025, 0.0375, 0.050, 0.075, 0.100, 0.450 and 0.600 g l^{-1} , respectively, and then rapidly dried. The insert diagram is a plot of ΔAbs_{477} as a function of $[\text{AO7}]$ using the data in the main diagram. The solid line is the line of best fit calculated using Eq. (6), assuming $k_{\text{ads}}[\text{dye}] \approx (k_{\text{ads}}[\text{dye}] + k_{\text{des}})$, and the following optimised values for $\Delta\text{Abs}_{575}(\infty) (\propto [\text{TiO}_2\text{-dye}]_\infty)$ and k_{ads} of 1.41 and $1.48 \text{ l g}^{-1} \text{ min}^{-1}$, respectively.

for MB at pH 11, which is consistent with the different values for k_{ads} for these two systems reported above.

3.3. Photocatalytic destruction of dried MB and AO films

The kinetics of the photocatalysed bleaching of air-dried, cationic and anionic dyes adsorbed on titania are complex and not well studied [1]. As noted earlier, Julson and Ollis and co-workers have proposed a very effective kinetic model for dyes, such as AB9, AO7, RB5 and RB 19, adsorbed onto titania involving two first-order reactions coupled in series [1]. A key feature of this model is

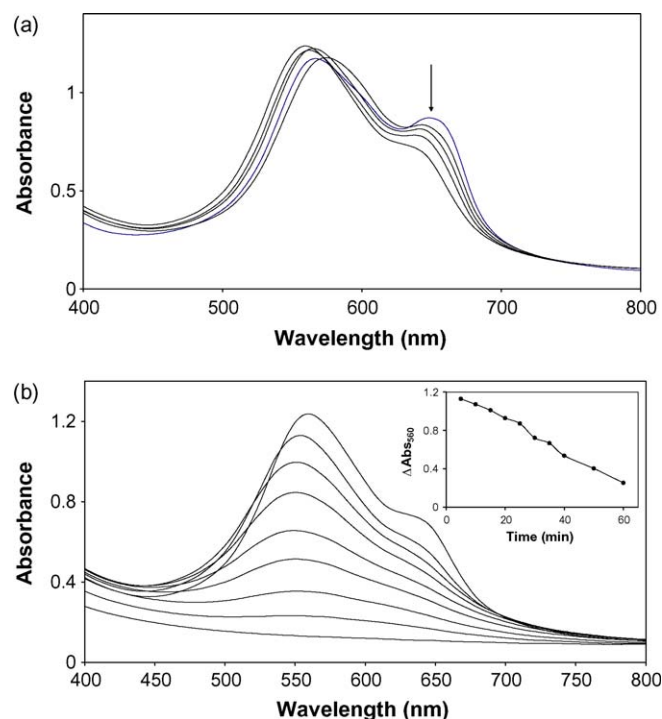


Fig. 6. Visible absorption spectra of MB (0.025 g l^{-1}) stained titania films (for 10 min) as a function of UVA irradiation time (a) for the first 5 min and (b) subsequently. For (a) at 660 nm the irradiation times are (from top to bottom): 0, 20, 60, 100 and 300 s, respectively. For (b) at 570 nm the irradiation times are (from top to bottom): 5, 15, 25, 30, 40, 50, 60, 70 and 95 min, respectively. The insert diagram is a plot of ΔAbs_{560} as a function of irradiation time, calculated using the data in (b).

that the intermediate – which refers to any and all light absorbing species not including the original dye itself – is formed from the dye via one first order process and decays to a colourless product via another (see Eq. (1)). Part of this study looks to see if this simple model is applicable to the photobleaching of examples of the cationic (MB) and anionic (AO7) stained mesoporous titania films.

Not surprisingly, given its apparent mixed oligomer composition, the most complex of the two dye systems studied is the photobleaching of MB-stained films at high pH, as illustrated in Fig. 6(a) and (b), for a titania film stained by soaking in a 0.025 g l^{-1} ($\approx 6.7 \times 10^{-5} \text{ M}$) MB solution at pH 11 for 10 min and irradiated using 5 mW cm^{-2} of UVA light. The kinetics are complex in that the first step, illustrated in Fig. 6(a), appears to be a rapid bleaching of the shoulder peak at 660 nm (within 5 min irradiation), accompanied by a shift in the position of the usual trimer peak at 570–560 nm. The lack of an isosbestic point shows that this initial bleaching process is not a simple conversion from one species to another and probably involves several processes and intermediate species. Since the peak at 660 nm is tentatively attributed to the J-aggregated dimer, the results in Fig. 6(a) indicate that this species is the first to be attacked, but probably not bleached. Instead, a very differently coloured intermediate product is generated, probably a demethylated form of MB, such as Azure B which has 3 methyl groups, instead of MB's four, and a λ_{max} at 648 nm in aqueous solution.

The demethylation of MB to form Azure B (and then possibly further demethylation to form Azure C, A and then thionine) as steps in the photocatalytic bleaching of MB in solution is well established [19,20] and likely to be the cause of the concomitant blue shift in the main absorption peak at 570 nm, *vide supra*. However, the lack of a clear isosbestic point indicates the conversion is not simple, and that some other, differently coloured, intermediates are formed at different rates. For irradiation times $>5 \text{ min}$ the observed spectral changes are more monotonic, as illustrated in Fig. 6(b) and the kinetics of bleaching, as measured by the change in absorbance at 560 nm, ΔAbs_{560} , are approximately zero-order; note: similar zero-order kinetics are observed using the same titania films to destroy multilayers of stearic acid [12]. Not surprisingly, these kinetics are very different from the first-order decays reported by most workers studying the photocatalysed bleaching of MB in aqueous solution using titania powders or films [3,15,19,20]. Not surprisingly, given the complex nature of the initial photo-induced spectral changes, the kinetics of dye photobleaching, whether measured at 650 or 570 nm, do not give a good fit to the simple kinetic model based on Eq. (1).

Interestingly, as the irradiation proceeds, the absorbance peak position at 560 nm gradually blue-shifts a further 10 nm, a feature that is associated with the further demethylation of MB as part of its photocatalytic destruction. In aqueous solution, using a titania powder, this blue shift is very large (typically ca. 54 nm) [19,20], thus, the small (10 nm) spectral shift observed in the photobleaching of MB indicates that the process of demethylation is less extensive for MB adsorbed on mesoporous titania films. QCM measurements carried out on the same system shows that dye bleaching occurs after ca. 83% of the time required for the mass loss due to the complete photo-oxidative mineralisation of the dye to volatile products. This finding is similar to the findings of Serpone et al. in their study of the photobleaching of MB in aqueous solution by titania powder particles who reported 90% TOC removal at the point when the solution was completely photobleached [20]. Both sets of results show that after dye bleaching the photocatalytic process continues until all the smaller, colourless organic species are completely mineralised to volatile inorganic species, such as CO_2 and water. Similar results were obtained using AO7.

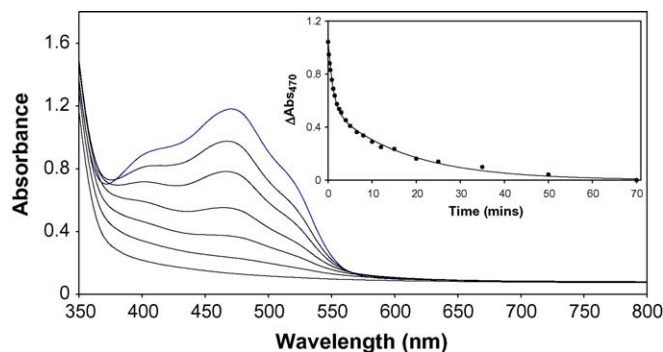


Fig. 7. Visible absorption spectra of AO7 (0.1 g l^{-1}) stained titania films (for 10 min) as a function of UVA irradiation time. The insert diagram is a plot of ΔAbs_{470} as a function of irradiation time, from the data in the main diagram. The solid line is the line of best fit to the data calculated using Eq. (7) and the optimised values for α , k_1 and k_2 of 0.49, 0.89 min^{-1} and 0.058 min^{-1} , respectively.

In contrast to the kinetics of MB photobleaching by a mesoporous titania film at high pH, under otherwise the same reaction conditions those for AO7 (0.1 g l^{-1} soaking solution, $\approx 2.85 \times 10^{-4} \text{ M}$) at low pH are simple as illustrated by the changing spectral profile as a function of irradiation time in Fig. 7. A plot of the change of absorbance of the AO7 film at its maximum (477 nm) as a function of irradiation time is illustrated in the insert diagram in Fig. 7. The fast initial decay and subsequent slow final bleaching step apparent from this plot is very similar to the decay profiles reported by Julson and Ollis for a variety of different dyes including AO7 on P25 titania [1].

The key kinetic expression relating absorbance $\text{Abs}(t)$ as a function of irradiation time, t , arising from the Julson–Ollis model [1] is as follows:

$$\text{Abs}(t) = \text{Abs}(t=0) \times \left(\left(\frac{\alpha k_1}{k_1 + k_2} \right) (\exp(-k_1 t) - \exp(-k_2 t)) + \exp(-k_1 t) \right) \quad (7)$$

where α is the ratio of the molar absorptivities of the intermediate and AO, and k_1 and k_2 are the first order constants for the two colour-degrading reactions coupled in series, see Eq. (1). Applying this equation to the observed variation in the absorbance of the AO7 film illustrated in the insert in Fig. 7 yields an excellent fit to the data as shown by the solid line which was calculated using Eq. (7) based on the optimised values for α , k_1 and k_2 of 0.49, 0.89 min^{-1} and 0.058 min^{-1} . For comparison, average values for α , k_1 and k_2 of 0.59, 0.11 and 0.0021, were reported by Julson and Ollis for the bleaching of AO7 on Degussa P25 TiO_2 powder [1], from which it is interesting to note that for the two systems the values of α are very similar and the values of k_1 and k_2 are not too dissimilar when the incident light intensity is taken into account (5 mW cm^{-2} in this work compared 1.3 mW cm^{-2} in the other work). Thus, it appears that the Julson–Ollis model [1] can be used to analyse the kinetics of dye photobleaching at the air–solid interface of dye-stained mesoporous titania films as well as powders for dyes for AO7 at least. It is likely that the model will extend to other dyes adsorbed on mesoporous films, provided the dyes are not adsorbed in a variety of different aggregated forms, as in the case of MB, since in the latter such systems the kinetics of dye bleaching are likely to be much more complex.

4. Conclusions

It is possible to alter markedly the extent of adsorption of charged dyes onto the surface of titania by adjusting the pH. Thus,

cationic and anionic dyes adsorb readily onto mesoporous titania films at high pH (pH 11) and low pH (pH 3), respectively, due to attractive coulombic forces, whereas these same dyes on the same films do not adsorb at pH 3 and 11, respectively, due to repulsive coulombic forces. The cationic dye, MB, adsorbs on mesoporous titania films at high pH as the trimer. Upon drying, although the trimer still dominates, there is an absorption peak at 665 nm, especially notable at low MB soaking solution concentrations, which could be due to the monomer, but more likely is the MB J-aggregate. In contrast, the product of the adsorption of the anionic dye, AO7, onto the mesoporous titania film at low pH has a spectrum very similar to that of the dye monomer. For both MB and AO7 the kinetics of adsorption are first order and yield high rate constants (3.71 and $1.48 \text{ l g}^{-1} \text{ min}^{-1}$), indicative of a strong adsorption process. Further evidence for this was the observation that both MB and AO7 stained films retained much of their colour when left overnight in dye free pH 11 and 3 solution, respectively. The kinetics of the photocatalysed bleaching of the air-dried MB–titania films are complex and are not well-described by the Julson–Ollis kinetic model [1]. Instead, there appears to be an initial fast but not simple demethylation step, followed by a gradual photobleaching accompanied by further demethylation. In contrast, the kinetics of photocatalytic bleaching of the air-dried AO7–titania film gives a good fit to the Julson–Ollis kinetic model, yielding values for the various fitting parameters not dissimilar to those reported by the latter authors [1]. Thus, it appears that this model is appropriate not only for dye bleaching on titania *powders* but also mesoporous *films*. Further work is needed to establish the full range of adsorbed species this model can be applied to when studying titania photocatalysis at the air–solid interface and the intermediates generated during the photobleaching process. The marked staining of titania films using cationic or anionic dyes

achieved by using high or low pHs, respectively, and their subsequent fairly rapid photobleaching provides a useful method of demonstrating the photocatalytic activity of titania (and probably most semiconductor photocatalytic oxides) powders and porous films.

References

- [1] A.J. Julson, D.F. Ollis, Appl. Catal. B 65 (2006) 315.
- [2] A. Mills, S.-K. Lee, J. Photochem. Photobiol. A: Chem. 152 (2000) 233.
- [3] A. Mills, M. McFarlane, Catal. Today 129 (2007) 22.
- [4] P. Sao Marcos, J. Marto, T. Trindade, J.A. Labrincha, J. Photochem. Photobiol. A: Chem. 197 (2008) 125.
- [5] A. Mills, J. Wang, A. Mills, J. Wang, J. Photochem. Photobiol. A: Chem. 182 (2006) 181.
- [6] V. Romeas, P. Pichat, C. Guillard, T. Chopin, C. Lehaut, New J. Chem. 23 (1999) 365.
- [7] B.N. Shelimov, N.N. Tolachev, O.P. Tkachenko, G.N. Baeva, K.V. Klementiev, A.Y. Stakheev, V.B. Kazansky, J. Photochem. Photobiol. A: Chem. 195 (2008) 81.
- [8] H. Kim, W. Choi, Appl. Catal. B: Environ. 69 (2007) 127.
- [9] P. Chin, D.F. Ollis, Catal. Today 123 (2007) 177.
- [10] H. Lachheb, E. Puzenat, A. Houas, M. Ksibi, E. Elaloui, C. Guillard, J.-M. Herrmann, Appl. Catal. B 39 (2002) 75.
- [11] K.C. Akrapotulu, C. Kordulis, A. Lycourghiotis, J. Chem. Soc. Faraday Trans. 86 (1990) 3437.
- [12] A. Mills, N. Elliott, G. Hill, D. Fallis, J.R. Durrant, R.L. Willis, Photochem. Photobiol. Sci. 2 (2003) 591.
- [13] R.W. Sabnis, Handbook of Acid–Base Indicators, CRC Press, Boca Raton, 2008.
- [14] F.J. Green, The Sigma–Aldrich Handbook of Stains. Dyes and Indicators, Aldrich Chemical Co., Milwaukee, 1991.
- [15] A. Houas, H. Lachheb, M. Ksibi, E. Elaloui, C. Guillard, J.-M. Herrmann, Appl. Catal. B 31 (2001) 145.
- [16] E. Braswell, J. Phys. Chem. 78 (1968) 2477.
- [17] K. Patil, R. Pawar, P. Talap, Phys. Chem. Chem. Phys. 2 (2000) 4313.
- [18] C. Guillard, E. Puzenat, H. Lachheb, A. Houas, J.-M. Herrmann, Int. J. Photoenergy 7 (2005) 1.
- [19] T. Zhang, T. Oyama, S. Horikoshi, H. Hidaka, J. Zhao, N. Serpone, Sol. Energy Mater. Sol. Cells 73 (2002) 287.
- [20] T. Zhang, T. Oyama, A. Aoshima, H. Hidaka, J. Zhao, N. Serpone, J. Photochem. Photobiol. A 140 (2001) 163.